A biologically inspired computational model relating vection and visually induced motion sickness: individual differences and sensitivity analysis

Ji J.T.T.[1], Chow E.[1], Lor F[1]., So R.H.Y.[1], Cheung R.[2], Stanney K.[3], and Howarth P.A.[4]

[1]Computational Ergonomics Research Team, Department of Industrial Engineering and Engineering Management, Hong Kong University of Science and Technology, Hong Kong SAR

[2]Department of Medicine, University of Hong Kong, Hong Kong SAR

[3]Industrial Engineering & System Management, University of Central Florida, Orlando, USA

[4]Department of Human Sciences, Loughborough University, England

[1]ieemjtt@ust.hk, [2]rtcheung@hku.hk, [3]stanney@mail.ucf.edu [4]p.a.howarth@lboro.ac.uk

Keywords: Biologically inspired; Computational model; Motion sickness; Vection; Simulation; Optokinetic drum.

Abstract. This paper presents a biologically inspired computational model that simulates the entire process from sensory stimuli to the occurrence of vection induced motion sickness. The model consists of three modules: (i) a visual-vestibular integration network of vection perception, (ii) a supervised-learning adaptation network, and (iii) a symptoms dynamic network. In this paper, we compare the predicted nausea ratings with published data and report how the model parameters can be tuned to account for individual variations of vection onset time, vection build-up time, level of saturated vection, and eventually the simulated levels of nausea. This paper contains preliminary data only.

Introduction

On average, about 30% of Chinese are susceptible to motion sickness (So *et al.*, 1999). The neural mismatch theory predicts that visual-vestibular integration, as the central mechanism of vection perception, is also essential for generating motion sickness (MS) (Reason, 1978). This predicted connection between vection and MS has been supported by empirical data (Hettinger et al., 1990). However, there have been recent debates on the role of vection in visually induced MS (VIMS) generations. On one hand, vection has been referred to as the sole cause of VIMS in many studies involving optokinetic drums (Hu et al., 1997, Hu & Stern, 1998, Stern et al., 1990, So and Lo, 1999; So *et al.*, 2001). On the other hand, researchers have proposed that vection is not the only factor that can cause VIMS (Flanagan et al., 2002). Furthermore, vection has been successfully dissociated with changes of VIMS severity levels when the field-of-view is restricted (Webb & Griffin, 2003). The authors propose that developing mathematical models substantiate explain and simulate the generation of vection induced motion sickness could be a useful addition to the recent healthy debate. In particular, if the model's structure is consistent with biological fact on visual and vestibular interactions. The authors humbly admit that the development of mathematical models to simulate VIMS is not new. Both Oman (1982, 1990) and Bos and Bles (1998) have reported models concerning MS. Unfortunately, the emphases of their model were not on vection. In this paper, we attempt to fill up this research gap by constructing a computational model which can reinforce the connection between

vection and MS. It has to be noted that it is not the intention of the authors to argue that vection is the only cause of MS, in fact, the authors also develop a biologically inspired model to explain OKN induced VIMS. The objective of this study is to further the understanding of the cause of VIMS through model development. Currently, the authors believe that VIMS is polysymptomic and are caused by multi-factors associated with visual and vestibular interactions. It is the conviction that if vection is indeed not a cause of VIMS, as the model becomes more and more biologically accurate, it will demonstrate the disassociation between VIMS and vection.

Initially, we set the scope of the model parameters to explain vection induced motion sickness generated inside an optokinetic drum rotating at constant velocity. Theoretically, the model can be generalized to other visual stimuli. Since evidence exists that vection is not the sole causal factor of VIMS, assumptions have been made to isolate the effect of vection on MS from the influence of other factors. First, we assume that OKN is fully suppressed by eye fixation to isolate effect of vection from optokinetic nystagmus (OKN). Second, we assume that head movement is fully constrained by head fixation and the rostrocaudual axis of head is carefully aligned along the earth-vertical axis to isolate effect of vection from subjective-vertical conflict (SVC). Third, we assume that head fixed human participant can use external instruments to stabilized his/her bodies, e.g., use hand holders or sit in a chair, for the purpose to isolate effect of vection from postural instability (PI).

Model development

Neural basis roadmap of vection-induced motion sickness. The neural basis of vection induced motion sickness is illustrated in Figure 1. A visual-vestibular sensory convergence terminal, consisting of brainstem, thalamus and human homologue of parietal-insular vestibular cortex (PIVC), converges signals about visual motions with respect to the retina and vestibular signal about head movement with respect to the earth (Guldin & Grusser, 1998; Brandt, 1999). This convergence terminal will then produce the perceived self-motion velocity and pass the self-motion signals to cerebellum via the brainstem. The cerebellum, a specialized organ for supervised learning to facilitate VIMS protective adaptation, is capable of generating corresponding sensory prediction output and produce neural mismatch signals as self-modification error signals. This mismatch signals can trigger the vestibulo-autonomic circuitry via the vestibular nuclei and directly mediates elicitation of VIMS symptoms such as nausea (Doya, 1999; Balaban & Porter, 1998). In the light of Reason's neural mismatch model, we proposed that the perceived self-motion velocity is the sensory signal directly contributing to vection induced motion sickness.

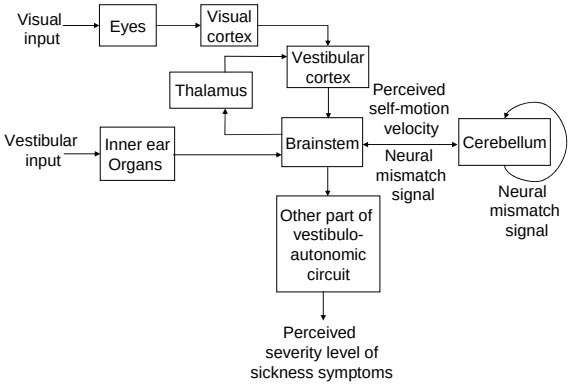

Figure1. Neural basis of vection induced MS inferred from neuroscience literatures (adopted from Ji *et al.,* 2008).

Conceptual model of vection induced motion sickness. Base upon the neural basis of vection induced MS, a three-module architecture is proposed. As illustrated in Figure2, Module1 (M1) is a visual-vestibular sensory integration network converging visual signals with vestibular signals.

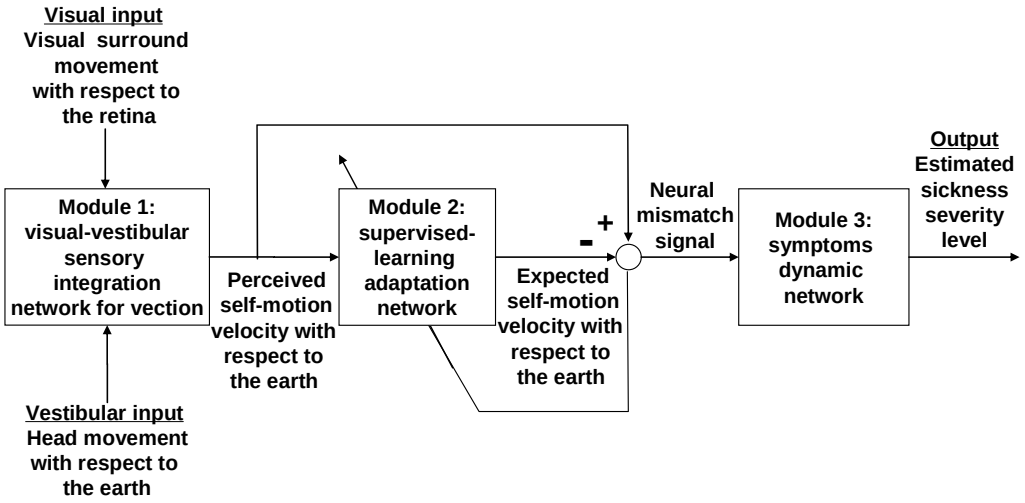

Figure 2. Three-module conceptual model of vection-induced motion sickness (adopted from Ji *et al.,* 2008).

Module2 (M2) is a supervised-learning adaptation network simulating the function of the cerebellum, It receives the perceived self-motion velocity and generates the optimal sensory prediction and neural mismatch signals. Module3 (M3) is a Stevens' power law-based symptoms dynamic network to estimate subjective sickness severity levels.

Computational model of vection-induced motion sickness: variable defintions. In this computational model, sensory input variables are: (i) rotating peripheral visual motion velocity with respect to the earth ω_{vis} (+ve means rotating to the left of the viewer), (ii) vestibular signals representing the head rotating velocity with respect to the earth ω_{vest}. Other variables include: the perceived self-rotating velocity with respected to the earth (ω_{per}), the expected or predicted self-rotating velocity with respected to the earth (ω_{exp}), and the neural mismatch signal (ω_{mis}). The model output, the estimated subjective nausea severity levels (O_{nausea}) is a non-negative scalar.

M1. Telban and Cardullo (2001)'s visual and vestibular interaction model has been modified and adopted in M1. In the original model proposed by Telban & Cardullo (2001), there is a weighting function K for the visual input and it's value varies between 0 and 1. This range of K forces the perceived self-motion velocity to reach a level of saturated vection given enough exposure time. In real life, however, some participants didn't experience vection saturation during exposure to rotating optokinetic drum (Stern *et al.*, 1990; Danieli *et al.*, 1996). Therefore, we modified the function of K by adding a parameter Φ to account for this individual differences on human vection perception as shown in Equation 1:

$$K = \Phi \cos\frac{\pi}{\xi}\omega_{err} + \Phi \cdot \qquad (1)$$

where Φ is the newly added parameter and has a value between 0 and 0.5. The weighting K in our model varies in a range from 0 to 2 Φ. The yaw direction vestibular indifference motion threshold ξ and the perceived conflict measure ω_{err} is defined according to Telban & Cardullo (2001).. The output of M1 is the time series data of

the perceived self-rotating velocity ω_{per} which serves as the input to M2, a supervised learning adaptation network.

M2. This module consists of a supervised-learning adaptive filter composed of a least mean square (LMS) adaptive linear neural network (ADALINE) with a tapped unit delay line to facilitate the predictive ability. First, the sampled input signal ω_{per} is transformed into a M-dimension input vector $U = [u_1, u_2, ..., u_M]^T$ using a sequence of unit delay functions ($\widetilde{D} = [1, D, ..., D^{M-1}]^T$) as shown in Equation 2:

$$U = \widetilde{D}\omega_{per} . \quad (2)$$

Referring to the cerebellar neural circuit proposed by Doya, 1999, the mossy fiber-granule cells input network cooperating with attached Golgi cells can realize the delaying function in the tapped unit delay line $\widetilde{D}$. The prediction output of this supervised-learning adaptive filter ω_{exp} is a linear combination of the M components of U weighted by a tunable weighting vector $W = [w_1, w_2, ..., w_M]^T$ plus a tunable bias b as shown in Equation 3:

$$\omega_{\exp} = U'W + b . \quad (3)$$

The prediction output signal ω_{exp} is a representation of Purkinje cell output formed by gathering parallel fiber signals $u_1, u_2, ..., u_M$ together through synaptic connections with different strengths ($w_1, w_2, ..., w_M$). Consequentially the neural mismatch signal ω_{mis} can be calculated by Equation 4:

$$\omega_{mis} = \omega_{per} - \omega_{\exp} . \quad (4)$$

The inferior olivary nucleus (ION) in the brainstem can work as the comparator of the input ω_{per} passed from the vestibular nuclei and the Purkinje cell prediction output ω_{exp} to compute the neural mismatch signal ω_{mis}. ω_{mis} is then fed back to the computation loop of prediction output ω_{exp} in an iterative manner to make ω_{exp} adapting towards ω_{per} and eventually to equal to ω_{per}. This convergence of prediction output and input is achieved by adjusting the components of weighting vector $W = [w_1, w_2, ..., w_M]^T$ and the bias b whose initial values are all zero and step changes dW and db are governed by LMS learning rule (Widrow & Hoff, 1960) as shown in Equation5:

$$\begin{cases} dW = lr\omega_{mis}U \\ db = lr\omega_{mis} \end{cases} . \quad (5)$$

where lr is the learning rate of the LMS adaptive filter. This adatptive network is consistent with the cerebellar neural circuit (Doya, 1999). Therefore the output of M2 ω_{mis} can serve as the input of M3, a symptom dynamic network.

M3. Oman (1982)'s nausea path dynamic model has been modified and adopted to implement M3. It takes in the neural mismatch or sensory conflict signal (ω_{mis}) and output the estimated subjective nausea severity levels (O_{nausea}). It is worth to point out that sensory conflict weighting in the nausea path dynamic module in the original Oman;s model is not adopted because the input to M3 (ω_{mis}) is already a sensory signal integrated from the weighted visual and vestibular input. Therefore in our model the M3 input ω_{mis} is directly rectified by Equation 6:

$$\widetilde{\omega}_{mis} = |\omega_{mis}| / c . \quad (6)$$

where c is a positive constant and $\widetilde{\omega}_{mis}$ is a the pre-processed neural mismatch signal. $\widetilde{\omega}_{mis}$ is passed into two parallel, interacting pathways to estimate the fast response and slow response of sickness response. Finally, the Stevens' power law equation is used to transform the sickness response to rated nausea levels.

Model simulation. Figure 3 shows a block diagram of the biologically inspired computational model of vection induced MS. The model is implemented by the Matlab-Simulink@ software package and a fourth-order variable-step Dromand -Prince algorithm is used for the simulation (the ode45 function in Simulink). The default

values used are: ϕ=0.35, M=5, lr=2^{-8}, c=60, k=0.8, I_0=0.05, a=0.96, and b=0.65. These values have been determined through a process of trial and error and with references to the literature where appropriate.

Compraing the predicted output with published data. Time course data of mean subjective nausea severity in the "eye-fixation" condition reported by Stern et al. (1990) is used as the benchmark of model prediction. The two model inputs are ω_{vis}= -60dps and ω_{vest}= 0dps. As illustrated in Figure 4, the model predicted time course of mean subjective nausea severity is enclosed in the 95% confidence interval (CI) envelop calculated from the empirical data. Although the predicted results are closed to the published empirical data, the authors acknowledge that the comparison has some shortcomings. First, nausea data were not collected as ratio scale data in Stern's study. Second, the model should be validated under more than one velocity condition. Therefore, stimulations shown in this section can at best be considered as a demonstration of predictive ability of the model. A review of literature indicates that suitable ratio scale nausea data with VIMS studies cannot be found. Currently, experiments are being conducted by the authors and initial results should be available for presentation at the symposium.

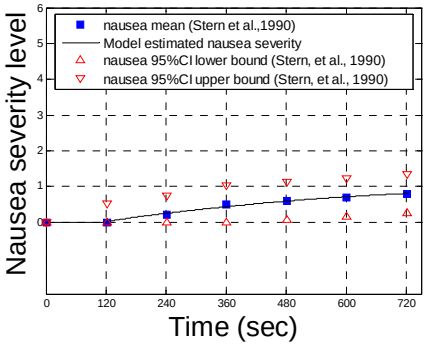

Figure 4. Predicted and empirically reported time courses data on mean subjective nausea severity levels of the "eye-fixation" condition in Stern et al. (1990). The distance between a pair of triangles for each 2mins represents size of the 95%CI calculated from empirical data. The solid line is model prediction. The square represents means of empirically collected data (adopted from Ji *et al.*, 2008).

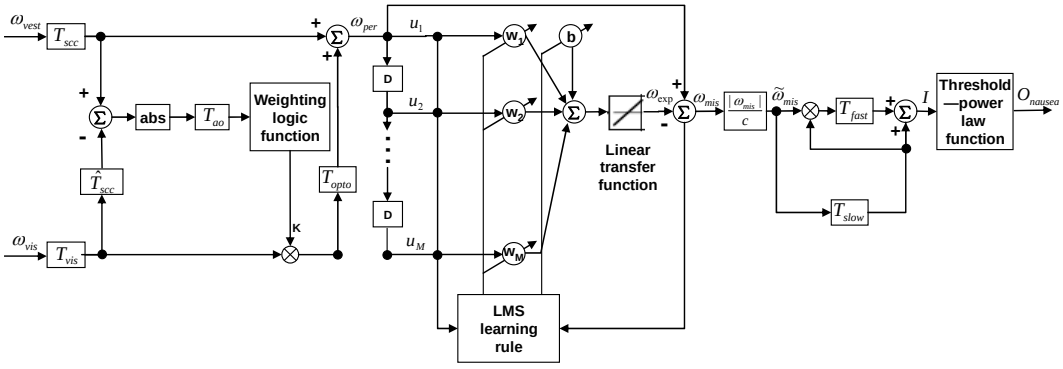

Figure 3. Block diagram of the biologically inspired computational model of vection-induced motion sickness (adopted from Ji *et al.*, 2008)

Individual differences and model sensitivity analysis

Large individual differences on vection onset, vection build-up time, and vection saturated level have been reported (Brandt *et al.*, 1973; Stern *et al.*, 1990). Our model can simulate individual difference on vection onset by tuning parameter τ_w and ξ. τ_w is time constant of transfer function $T_{\omega o}$ which is a high pass filter used to wash out the high-frequency mismatch between visual input and vestibular input over time. ξ is a preset parameter in weighting logic function K and defined to equal the mean yaw direction vestibular indifference motion threshold. Vection onset is positive correlated with τ_w and negatively correlated with ξ. It was reported that ξ varies in a range of 0.84 to 4.63dps for different human individuals (Benson *et al.*, 1989). However, model simulation shows that vection onset change caused by this variation is less than 0.5 sec. Therefore, we simply use an adjustable τ_w to account for a hypothetical variation of vection onset time from 3 to 5 sec in our model.

Likewise we can simulate individual difference on vection build-up time by tuning parameter τ_{va} which is a time constant of transfer function T_{opto} (Figure 3) accounting for the low pass frequency response of vection. Simulated results indicated that vection build-up time increases with increasing τ_{va}. Therefore, we can use an adjustable τ_{va} to account for a hypothetical variation of vection build-up time from 7 to 10secs in our model. Similarly, we can simulate individual difference on vection saturated level by tuning parameter Φ in weighting logic function K. Vection saturated level increases linearly along with increase of Φ. Therefore we can use an adjustable Φ to account for a hypothetical variation of vection saturated level from 36 to 48dps.

Our sensitivity analysis shows that, among the three types of individual differences on vection perception, only model simulated variation of vection saturated level contributes part of the variance of subjective nausea severity reported empirically. Results indicated that a 33% change of model simulated vection saturated level accounts for about 10% of the total variance. This result is consistent with the moderate correlation between vection and motion sickness observed from empirical study (Hettinger *et al.*, 1990). Although model simulated sickness is directly triggered by the perceived self-motion velocity, the effect of vection can be modulated by effects of other individual differences, e.g., motion sickness susceptibility (Reason and Brandt, 1975). Several model parameters can be adjusted to account for this motion sickness susceptibility variation, e.g., learning rate lr in M2, threshold I_0, gains and time constants of fast and slow dynamic elements in M3. The ability of this model to account for individual differences is an important contribution.

Conclusion

This paper presents a biological inspired computational model simulating the process of vection induced motion sickness elicitation. Model simulation produce predicted rated nausea levels that are comparable to those published in Stern *et al.* (1990). In addition, the model has been shown to be able to simulate individual variations in VIMS responses as well. In particular, the model can account for individual differences in vection onset time, vection build-up time, vection saturated levels, and rated nausea levels. Among other side-effects associated with a virtual reality system (e.g., time delays: So and Griffin, 1991, 1992, 2000; So and Chung *et al.*, 1999), motion sickness has been the one that has caused major concerns (Kiryu and So, 2007; Lo and So, 2001). The model reported in this paper is an important step towards the

development of a sickness-free virtual reality simulation.

Acknowledgments

The authors would like to thank the Hong Kong Research Grants Council for grants 615404E and 619907 and DAG05/06.EG20.

References

Balaban, C.D. and Porter, J.D. (1998) Neuroanatomic substrates for vestibulo-autonomic interactions. Journal of Vestibular Research, 8, pp.7-16.

Benson, A.J., Hutt, E. C. B., and Brown, S. F. (1989).Thresholds for the perception of whole body angular movement about a vertical axis. Aviation, Space, and Environmental Medicine, 60, pp.205-213.

Bos, J.E. and Bles, W. (1998) Modelling motion sickness and subjective vertical mismatch detailed for vertical motions. Brain Res Bull, 47, pp.537-42.

Brandt, T., Dichgans, J., and Koenig, E. (1973) Differential effects of central versus peripheral vision on egocentric and exocentric motion perception. Exp. Brain Res, 16:476-491

Brandt, T. (1999) "Vestibular cortex: its locations, functions, and disorders" in Vertigo. In: Springer, pp.219-230.

Danieli B.; Lesma G.; Passarella D.; Silvani A.; Kennedy R.S.; Hettinger L.J.; Harm D.L.; Ordy J.M. and Dunlap W.P.(1996) Psychophysical scaling of circular vection (CV) produced by optokinetic (OKN) motion: individual differences and effects of practice. Journal of Vestibular Research, 6, pp.331-341.

Doya, K. (1999) What are the computations of the cerebellum, the basal ganglia and the cerebral cortex? Neural Networks, 12, pp.961–974.

Flanagan, M.B., May, J.G. and Dobie, T.G. (2002) Optokinetic nystagmus, vection, and motion sickness. Aviation, space and environmental medicine, 73, pp.1067-73.

Guldin, W.O. and Grusser, O.J. (1998) Is there a vestibular cortex? Trends in Neurosciences, 21, pp. 254-259.

Hettinger, L.J., Berbaum, K.S., Kennedy, R.S., Dunlap, W.P., & Nolan, M.D. (1990) Vection and simulator sickness. Military Psychology, 2, pp.171-181.

Hu, S., Davis, M.S., Klose, A.H., Zabinsky,E.M., Meux,S.P., Jacobsen,H.A., *et al*. (1997) Effects of spatial frequency of a vertically striped rotating drum on vection-induced motion sickness. Aviat Space Environ Med, 68, pp.306-311.

Hu, S. & Stern, R.M. (1998) Optokinetic nystagmus correlates with severity of vection-induced motion sickness and gastric tachyarrhythmia. Aviat Space Environ Med., 69, pp.1162-1165.

Ji, J.T.T., So, R.H.Y., Lor, F. & Cheung, R. (2008) A heuristics time-series computational model to predict visually induced motion sickness as correlates of retinal slip velocity and vection perception. Awaiting publication.

Kiryu, T. and So, R.H.Y. (2007) Sensation of Presence and Cybersickness in applications of Virtual Reality for Advanced Rehabilitation. Journal of NeuroEngineering and Rehabilitation, 4:34.

Lo, W.T. and So, R.H.Y., (2001) Cybersickness in the presence of scene rotational movements along different axes. Applied Ergonomics, Vol.32, No.1, 2001, pp. 1-14.

Oman, C.M. (1982) A heuristic mathematical model for the dynamic of sensory conflict and motion sickness. Acta Otolaryngol Supplementum, 392, pp.5-44.

Oman, C.M. (1990) Motion sickness: a synthesis and evaluation of the sensory conflict theory. Canadian Journal of Physiology and Pharmacology, 68, pp.294-303.

Reason, J.T. (1978) Motion sickness adaptation: a neural mismatch model. J. R. Soc. Med, 71, pp.819-829.

Reason, J.T. and Brand. J.J.(1975) Motion sickness. Imprint London ; New York : Academic Press.

So, R.H.Y., Chung, K.M. and Goonetilleke, R.S. (1999) Target-directed head movements in a head-coupled virtual environment: predicting the effects of lags using Fitts' law. Human Factors, Vol.41, No.3, 1999, pp. 474-486.

So, R.H.Y., Finney, C.M. and Goonetilleke, R.S. (1999) Motion sickness susceptibility and occurrence in Hong Kong Chinese." Contemporary Ergonomics 1999, Taylor & Francis. pp.88-92.

So, R.H.Y. and Griffin, M.J. (1991) Effects of time delays on head tracking performance and the benefits of lag compensation by image deflection." Proceedings of Flight Simulation Technologies Conference, New Orleans, Louisiana, 12-14 August, 1991, pp.124-130.

So, R.H.Y. and Griffin, M.J. (1992), Compensating lags in head-coupled displays using head position prediction and image deflection. J. Aircraft. 29(6): 1064-1068, 1992.

So, R.H.Y. and Griffin, M.J. (2000) Effects of target movement direction cue on head-tracking performance. Ergonomics, Vol.43, No.3, pp. 360-376.

So, R.H.Y. and Lo, W.T. (1999) Cybersickness: An Experimental Study to Isolate the Effects of Rotational Scene Oscillations. Proceedings of IEEE Virtual Reality '99 Conference, March 13-17, 1999, Houston, Texas. Published by IEEE Computer Society, pp.237-241.

So, R.H.Y., Lo, W.T. and Ho, A.T.K., (2001) "Effects of navigation speed on the level of cybersickness caused by an immersive virtual environment". Human Factors, 43, pp.452-461.

Stern, R.M., Hu, S., Anderson, R.B., Leibowitz, H.W. and Koch, K.L. (1990) The effects of fixation and restricted visual field on vection-induced motion sickness. Aviat Space Environ Med, 61, pp.712-715.

Telban, R.J. and Cardullo, F.M. (2001) An integrated model of human perception with visual-vestibular interaction. American institute of aeronautics and astronautics (AIAA) Modeling and Simulation Technologies Conference and Exhibit, Montreal, Canada, Aug. 6-9, 2001

Webb, N.A. and Griffin, M.J. (2003) Eye movements, vection and motion sickness with foveal and peripheral vision. Aviat Space Environ Med, 74, pp.622-625.

Widrow, B. and Lehr, M.A. (1990) 30 years of adaptive neural networks: perceptron, Madaline, andbackpropagation. Proceedings of the IEEE, 78, pp.1415-144.